Elastic modulus of amorphous SiO 2 nanowires

Hai Ni, Xiaodong Li, and Hongsheng Gao

Citation: Applied Physics Letters **88**, 043108 (2006); doi: 10.1063/1.2165275
View online: http://dx.doi.org/10.1063/1.2165275
View Table of Contents: http://scitation.aip.org/content/aip/journal/apl/88/4?ver=pdfcov
Published by the AIP Publishing

Elastic modulus of amorphous SiO_2 nanowires

Hai Ni, Xiaodong Li,[a] and Hongsheng Gao
Department of Mechanical Engineering, University of South Carolina, 300 Main Street, Columbia, South Carolina 29208

(Received 17 October 2005; accepted 7 December 2005; published online 25 January 2006)

Amorphous SiO_2 nanowires with diameter ranging from 50 to 100 nm were synthesized using chemical vapor deposition (CVD) under an argon atmosphere at atmospheric pressure. Nanoscale three-point bending tests were performed directly on individual amorphous SiO_2 nanowires using an atomic force microscope (AFM). Elastic modulus of the amorphous SiO_2 nanowires was measured to be 76.6 ± 7.2 GPa, which is close to the reported value of the bulk SiO_2 and thermally grown SiO_2 thin films, but lower than that of plasma-enhanced CVD SiO_2 thin films. The amorphous SiO_2 nanowires exhibit brittle fracture failure in bending. © *2006 American Institute of Physics*. [DOI: 10.1063/1.2165275]

One-dimensional (1D) nanomaterials have been found to possess remarkable properties, such as electrical, optical, catalytic, and mechanical properties.[1–6] These intriguing properties of 1D nanomaterials offer great opportunities to use them as potential functional and structural nanobuilding blocks in nanoscale electronic, optical, bioengineering, and micro/nanoelectromechancial systems applications, and have triggered great efforts to synthesize various 1D nanomaterials, such as tubes and/or wires of C,[4,7–10] B,[11–13] Si,[14–16] SiO_2,[17–19] and GaN,[20–22] to name a few.

As one of the most important photoluminescence materials, SiO_2 has been widely used in the electronic industry.[17] Recently, SiO_2 nanowires have shown a great promise as functional and structural nanobuilding blocks in nanoelectronics. Various methods, such as chemical vapor deposition (CVD),[18,23–25] laser ablation,[26] sol-gel,[27] and thermal evaporation methods,[28] have been used to produce SiO_2 nanowires on a large scale, from well-aligned to nanoflower morphology.[18,19] In order to integrate these nanowires into functional nanodevices, a precise measurement of the mechanical properties is of significant importance, because mechanical failure of these nanobuilding blocks may lead to the malfunction or even fatal failure of the entire devices.

Recent studies have revealed that material properties are size dependent. The extremely small dimensions of 1D nanomaterials impose a tremendous challenge to many existing testing and measuring techniques for experimental studies of their mechanical properties. An atomic force microscope (AFM), having high spatial resolution and force sensing capabilities, has been proven to be a robust mechanical property characterization tool for 1D nanomaterials. The AFM combined with a nanoindenter was used to measure the mechanical properties of silver nanowires,[29] ZnS nanobelts,[30] and Cu_2O nanocubes.[31] The AFM contact mode was used to extract the elastic modulus from the force-deflection response of carbon nanotubes[32,33] and silicon nanowires.[34] Recently, the AFM lateral force mode was used to bend gold nanowires in order to determine the elastic modulus and fracture strength.[35] To date, the mechanical properties of SiO_2 nanowires are still lacking. This has limited their applications in constructing reliable nanodevices.

In this study, amorphous SiO_2 nanowires were synthesized using CVD via a vapor-liquid-solid method, after characterizing their microstructure and composition using various electron microscopy techniques, we measured the elastic modulus of the amorphous SiO_2 nanowires by directly bending individual suspended wires using an AFM tip. This letter also reports a reliable nanowire clamping technique for the manipulation and mechanical testing of 1D nanomaterials.

The amorphous SiO_2 nanowires were synthesized using CVD through a vapor-liquid-solid method. During the synthesis, high-purity argon flow rate varied from 50 to 270 sccm (standard cubic centimeters per minutes), through a three-zone tube furnace with temperature control for each zone. Silicon powder (99.995% pure) was used as source material and was placed near the center of the furnace with a temperature of 1075 °C. The silicon (100) wafer with a 20 nm gold coating was used as the substrate and placed near the lower-temperature zone (900 °C) and downstream of the argon flow. After holding 30 to 60 min at the controlled temperature, the nanowires were removed from the tube furnace and immediately examined by scanning electron microscopy (SEM) (FEI Quanta 200), energy dispersive x-ray (EDX) spectroscopy, and transmission electron microscopy (TEM) (Hitachi H-8000).

The nanowire containing solution was dropped onto a standard AFM reference sample (Veeco Metrology Group) with uniform channels. In order to avoid nanowire sliding during the bending tests, both ends of the nanowires, which bridged the channel, were clamped by electron-beam-induced deposition (EBID) of carbonaceous materials (paraffin).[36] A Veeco Dimension 3100 AFM was used to perform three-point bending tests by directly indenting the center of a suspended nanowire which bridged the channel with a tapping mode silicon AFM tip.

Figure 1(a) shows the SEM image of the as-grown SiO_2 nanowires. EDX analysis, seen in Fig. 1(b), clearly shows that only oxygen and silicon exist except a small peak from gold catalyst. Figures 1(c) and 1(d) show the low and high magnification TEM images of the assynthesized nanowires. One can clearly see the general morphology of the nanowires: The surface is smooth and free of defects, the microstructure is homogeneous, and the nanowires have a high purity. The individual nanowires are uniform with diameter ranging from 50 nm to100 nm. The TEM selected area elec-

[a]Author to whom correspondence should be addressed; electronic mail: lixiao@engr.sc.edu

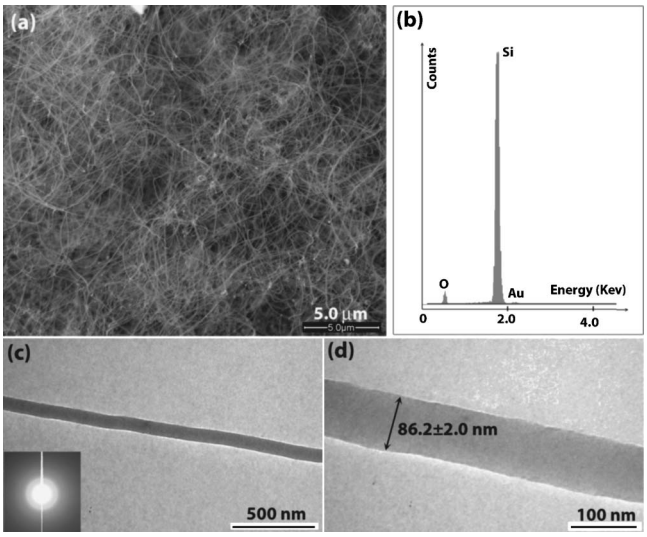

FIG. 1. (a) SEM image showing the morphology of the as-synthesized SiO_2 nanowires and (b) the corresponding EDX result, (c) low and (d) high magnification TEM images showing the morphology of the as-synthesized SiO_2 nanowires. The inset shows a highly diffuse electron diffraction ring pattern, indicating amorphous structure of the as-synthesized SiO_2 nanowires.

tron diffraction pattern [inset in Fig. 1(c)] shows that no spot pattern was observed except highly diffuse rings. This clearly indicates that the as-grown nanowires are amorphous in nature.

The SiO_2 nanowires containing solution was dropped onto the surface of the Veeco 3D reference standard sample, and the reference sample was then examined in the SEM for locating nanowires, which bridged well over the trenches. Both ends of the suspended nanowires were further clamped by the EBID process. Figure 2(a) shows such a well aligned, suspended SiO_2 nanowire over a trench. By examining the carbon peaks in Figs. 2(b) and 2(c), one can clearly see that after a 2 min EBID, a significant amount of carbonaceous

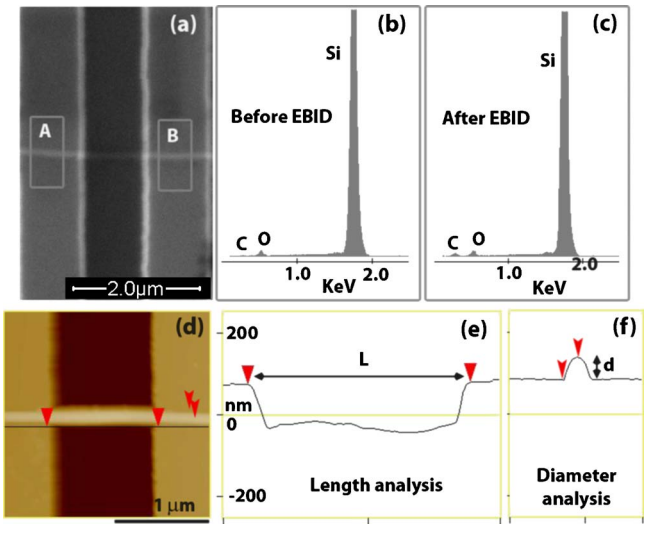

FIG. 2. (Color online) (a) SEM image showing a three-point bending SiO_2 nanowire sample bridging a 1 μm wide trench, and both ends of the wire were clamped to the substrate by EBID of carbonaceous materials, (b) EDX result from Frames A and B showing the almost absence carbon peak before EBID, and (c) EDX result from Frames A and B showing an obvious carbon peak after EBID, which indicates a layer of carbonaceous material was deposited within the Frame A and B after 2 min EBID. (d) AFM image of a suspended nanowire and its corresponding height profile along (e) and across (f) the wire for the nanowire length and diameter determination.

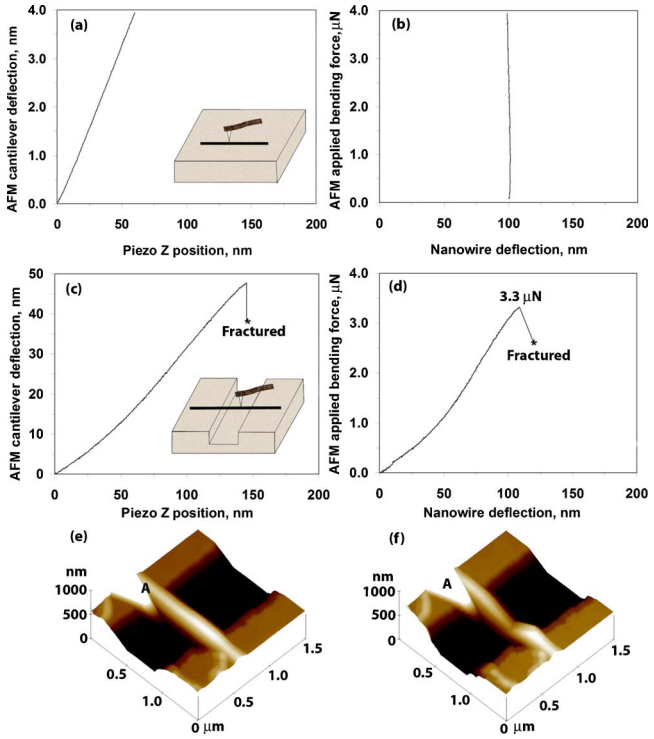

FIG. 3. (Color online) (a) Cantilever and (b) nanowire deflections obtained by directly indenting a SiO_2 nanowire sitting on a solid Si substrate. (c) Cantilever and (d) nanowire deflections obtained on a suspended SiO_2 nanowire. (e) and (f) 3D AFM images showing the suspended SiO_2 nanowire morphology before and after three-point bending testing corresponding to (c) and (d), respectively. The nanowire fractured in a brittle manner at a bending force of 3.3 μN. Note: Area "A" was dirt.

material has been deposited onto the surface within the frames shown in Fig. 2(a). As can be seen later, this thin layer carbonaceous material and the adhesion force between the nanowire and the substrate are strong enough to anchor both ends of the suspended SiO_2 nanowire during indentation bending. Thus, the suspended SiO_2 nanowire can be treated as a double clamped beam.

Before performing each three-point bending test, an AFM image—together with its height profiles both along and across the nanowire—was obtained, as shown in Figs. 2(d)–2(f), and used to determine the suspended length and diameter of each nanowire to be tested.

The measured total deflection (d_t) is composed of two components: The deflection from the cantilever (d_c) and the deflection from the nanowire (d_n). In order to avoid penetration of the AFM tip into the nanowire during three-point bending testing, the maximum applied load, below which no or negligible amount of penetration occurs, should be identified. We performed an AFM indentation test directly on a SiO_2 nanowire sitting on a silicon substrate, as shown in Figs. 3(a) and 3(b). At a 4 μN indentation force, the penetration of the AFM tip into the nanowire, i.e., the nanowire deflection shown in Fig. 3(b), was within range of ±1 nm after subtracting the cantilever deflection. This force was the maximum applied load used in all three-point bending tests in this study.

Figure 3(c) shows the AFM cantilever-piezo position along the z-direction curve for a suspended SiO_2 nanowire under an applied bending force of 3.3 μN until fracture failure, and the corresponding applied force-nanowire deflection relationship is shown in Fig. 3(d). As one can see, the ap-

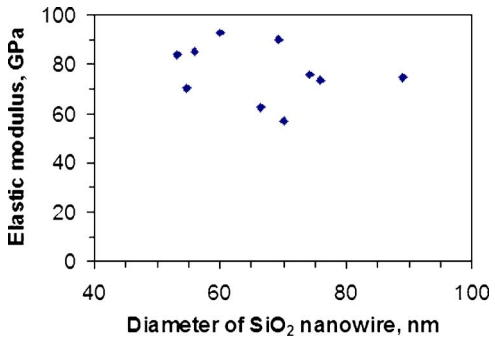

FIG. 4. (Color online) Bending elastic modulus of the amorphous SiO_2 nanowire vs nanowire diameters.

plied force and nanowire deflection keeps a very good linear relationship up to 1 μN, and then shows a slightly nonlinear relationship until final catastrophic failure occurs. This phenomenon was also observed by Paulo *et al.*[34] on a double-clamped silicon nanobeam. In addition to the bending deflection, the stretching of the nanowire also contributes to the overall nanowire deflection under sufficiently large bending force, and this may change the initial linear relationship between the applied force and the nanowire deflection. The brittle fracture feature can be further verified from the 3D AFM image in Fig. 3(f) [the suspended nanowire before bending is shown in Fig. 3(e)]; as it shows almost no plastic deformation. The slope of the initial linear potion of the curve in Fig. 3(d) was calculated and treated as the spring constant of the nanowire. Based on the assumption that the nanowire follows the linear elastic theory of an isotropic material, the elastic modulus of the SiO_2 nanowire, E_n, can be calculated from[35,37]

$$E_n = FL^3/192d_nI = k_nL^3/192I, \quad (1)$$

where I is the moment of inertia. For a round-shaped nanowire, $I=\pi r^4/4$, where r is the radius of the nanowire, L is the suspended length of the nanowire, and F is the applied load at its midpoint position. $k_n(=F/d_n)$ is the spring constant of the nanowire.

For all tested nanowires with a diameter ranging from 50 nm to 100 nm, the calculated elastic modulus ranged from 57 to 93 GPa and the average elastic modulus is 76.6 ± 7.2 GPa, which is close to the reported value of 73 GPa of thermally grown SiO_2 thin films[38] and the bulk SiO_2,[39] but lower than that of plasma-enhanced CVD (PECVD) SiO_2 thin films.[40] For example, the highest reported elastic modulus of 144 GPa is from 1 μm SiO_2 thin film deposited by PECVD.[40] This discrepancy is probably due to the different synthesis processes and different testing techniques. Normally, the quality and density of PECVD SiO_2 differ from thermally grown SiO_2.[41,42] For SiO_2 thin films, the elastic modulus was found to be dependent upon thin-film synthesis processes. PECVD SiO_2 thin films usually exhibit a higher elastic modulus than thermally grown ones.[40] It can be seen from Fig. 4 that the elastic modulus of the amorphous SiO_2 nanowires is independent of the wire diameter in the range of 50–100 nm.

Financial support for this study from the National Science Foundation (Grant No. EPS-0296165), the ACS Petroleum Research Fund (ACS PRF No. 40450-AC10), and the University of South Carolina NanoCenter are highly appreciated.

[1] P. M. Ajayan, Chem. Rev. (Washington, D.C.) **99**, 1787 (1999).
[2] Y-T Cheng, A. M. Weiner, C. A. Wong, M. P. Balogh, and M. J. Lukitsch, Appl. Phys. Lett. **81**, 3248 (2002).
[3] S. B. Sinnott and A. Andrews, Crit. Rev. Solid State Mater. Sci. **26**, 145 (2001).
[4] S. Iijima, Nature (London) **354**, 56 (1991).
[5] U. Landman, W. D. Luedtke, N. A. Burnham, and R. J. Colton, Science **248**, 454 (1990).
[6] M. F. Yu, O. Lourie, M. J. Dyer, K. Moloni, T. F. Kelly, and R. S. Rouff, Science **287**, 637 (2000).
[7] W. Z. Li, S. S. Xie, L. X. Qian, B. H. Chang, B. S. Zou, W. Y. Zhou, R. A. Zhao, and G. Wang, Science **274**, 1701 (1996).
[8] A. A. Puretzky, D. B. Geohegan, X. Fan, and S. J. Pennycook, Appl. Phys. Lett. **76**, 182 (2000).
[9] C. R. Martin, Science **266**, 1961 (1994).
[10] H. W. Zhu, C. L. Xu, D. H. Wu, B. Q. Wei, R. Vajtai, and P. M. Ajayan, Science **296**, 884 (2002).
[11] C. J. Otten, O. R. Lourie, M. F. Yu, J. M. Cowley, M. J. Dyer, R. S. Rouff, and W. E. Buhro, J. Am. Chem. Soc. **124**, 4564 (2002).
[12] S. H. Yun, A. Dibos, J. Z. Wu, and D. K. Kim, Appl. Phys. Lett. **84**, 2892 (2004).
[13] J. Niu, J. Sha, X. Y. Ma, J. Xu, and D. Yang, Chem. Phys. Lett. **367**, 528 (2003).
[14] W. S. Shi, H. Y. Peng, Y. F. Zheng, N. Wang, N. G. Shang, Z. W. Pan, C. S. Lee, and S. T. Lee, Adv. Mater. (Weinheim, Ger.) **12**, 1343 (2000).
[15] Y. Yao, F. H. Li, and S. T. Lee, Chem. Phys. Lett. **406**, 381 (2005).
[16] J. D. Holmes, K. P. Johnston, R. C. Doty, and B. A. Korgel, Science **287**, 1471 (2000).
[17] B. Zheng, Y. Wu, P. Yang, and J. Liu, Adv. Mater. (Weinheim, Ger.) **14**, 122 (2002).
[18] J. Q. Hu, Y. Jiang, X. M. Meng, C. S. Lee, and S. T. Lee, Chem. Phys. Lett. **367**, 339 (2003).
[19] Y. Q. Zhu, W. K. Hsu, M. Terrones, N. Grobert, H. Terrones, J. P. Hare, H. W. Kroto, and D. R. M. Walton, J. Mater. Chem. **8**, 1859 (1998).
[20] G. S. Cheng, L. D. Zhang, X. G. Zhu, S. H. Chen, Y. Li, Y. Zhu, and G. T. Fei, Nanostruct. Mater. **11**, 421 (1999).
[21] G. S. Cheng, L. D. Zhang, Y. Zhu, G. T. Fei, L. Li, C. M. Mo, and Y. Q. Mao, Appl. Phys. Lett. **75**, 2455 (1999).
[22] G. Fasol, Science **272**, 1751 (1996).
[23] Z. Q. Liu, S. S. Xie, L. F. Sun, D. S. Tang, W. Y. Zhou, C. Y. Wang, W. Liu, Y. B. Li, X. P. Zou, and G. Wang, J. Mater. Res. **16**, 683 (2001).
[24] X. C. Wu, W. H. Song, K. Y. Wang, T. Hu, B. Zhao, Y. P. Sun, and J. J. Du, Chem. Phys. Lett. **336**, 53 (2001).
[25] J. Niu, J. Sha, N. Zhang, Y. Ji, X. Ma, and D. Yang, Physica E (Amsterdam) **23**, 1 (2004).
[26] D. P. Yu, Q. L. Hang, Y. Ding, H. Z. Zhang, Z. G. Bai, J. J. Wang, Y. H. Zou, W. Qian, G. C. Xiong, and S. Q. Feng, Appl. Phys. Lett. **73**, 3076 (1998).
[27] M. Zhang, Y. Bando, L. Wada, and K. Kurashima, J. Mater. Sci. Lett. **18**, 1911 (1999).
[28] C. H. Liang, L. D. Zhang, G. W. Meng, Y. W. Wang, and Z. Q. Chu, J. Non-Cryst. Solids **277**, 63 (2000).
[29] X. Li, H. Gao, C. J. Murphy, and K. K. Caswell, Nano Lett. **3**, 1495 (2003).
[30] X. Li, X. Wang, Q. Xiong, and P. C. Eklund, Nano Lett. **5**, 1982 (2005).
[31] X. Li, H. Gao, C. J. Murphy, and L. Gou, Nano Lett. **4**, 1903 (2004).
[32] J. Salvetat, A. Kulik, J. Bonard, G. Briggs, T. Stöckli, K. Méténier, S. Bonnamy, and F. Béguin, Adv. Mater. (Weinheim, Ger.) **11**, 161 (1999).
[33] B. Lukic, J. Seo, R. Bacsa, S. Delpeux, F. Béguin, G. Bister, A. Fonseca, J. Nagy, A. Kis, S. Jeney, A. Kulik, and L. Forró, Nano Lett. **5**, 2074 (2005).
[34] A. San Paulo, J. Bokor, R. Howe, R. He, P. Yang, D. Gao, C. Carraro, and R. Maboudian, Appl. Phys. Lett. **87**, 053111 (2005).
[35] B. Wu, A. Heidelberg, and J. J. Boland, Nat. Mater. **4**, 525 (2005).
[36] W. Ding, D. A. Dikin, X. Chen, R. D. Piner, R. S. Ruoff, E. Zussman, X. Wang, and X. Li, J. Appl. Phys. **98**, 014905 (2005).
[37] T. Namazu, Y. Isono, and T. Tanka, J. Microelectromech. Syst. **9**, 450 (2000).
[38] C. Tsou, Y. S. Huang, and H. C. Chang, NSTI-Nanotech. **3**, 339 (2005).
[39] B. Bhushan, *Handbook of Nanotechnology* (Springer, Berlin, 2004), p. 773.
[40] X. Li, B. Bhushan, K. Takashima, C.-W. Baek, and Y.-Y Kim, Ultramicroscopy **97**, 481 (2003).
[41] I. Idris and O. Sugiura, Jpn. J. Appl. Phys., Part 1 **37**, 6562 (1998).
[42] IEEE Trans. Electron Devices **25**, 1249 (1978).